Karaelmas Science and Engineering Journal
Journal home page: http://fbd.beun.edu.tr
DOI: 10.7212/zkufbd.v9i2.1324

Research Article
Received / Geliş tarihi : 10.04.2018
Accepted / Kabul tarihi : 08.05.2018

PQ Controller for Single Phase Bridgeless Boost PFC Rectifiers

Tek Fazlı Köprüsüz Yükseltici PFC Doğrultucular İçin PQ Kontroller

Yasemin Önal*

Bilecik Seyh Edebali University, Department of Electrical&Electronic Engineering, Bilecik, Turkey

Abstract

Nonlinear loads generate disturbances in the power grid, which impact the grid voltage quality. These also generate reactive power, which causes losses in the transmission and distribution systems. It needs to control the power quality of the grid as well as the power, due to the nonlinear loads. This research presents a new controller for Bridgeless Boost Power Factor Correction PFC (BBPFC) rectifiers to improve the Total Harmonic Distortion THD of the utility grid along with the power factor on the grid. The input rectifier bridge in conventional boost PFC(CBPFC) rectifiers are discarded in bridgeless rectifiers to reduce complexity and increase the overall efficiency. The P and Q powers are controled through inner current loop in the improved algorithm. The reference current is calculated in the inner control loop through innovative filtering and signal processing. The inner current loop generates PWM switching signals by using PI controller. Analytical resolution of the suggested technic of controller is presented in details. The performance of the controller which is advised is confirmed for 300W rectifier by using PSIM circuit simulations.

Keywords: Bridgeless boost rectifier, Power factor correction PFC, Power quality, Total harmonics distortion, PQ theory

Öz

Doğrusal olmayan yükler şebeke geriliminin kalitesini etkileyen harmonikler oluşturmaktadır. Hemde iletim ve dağıtım sistemlerinde kayıplara sebep olan reaktif güç üretmektedirler. Doğrusal olmayan yükler nedeniyle şebekenin güç faktörünün yanı sıra güç kalitesinin de kontrol edilmesi gerekmektedir. Bu araştırmada, şebekenin güç faktörünün yanı sıra toplam harmonik bozulma değerini (THB) iyileştirmek için kullanılan köprüsüz yükseltici güç faktörü düzelticileri (KYGFD) için yeni bir kontrol algoritması sunulmuştur. Karmaşıklığı azaltmak ve genel verimliliği artırmak için köprüsüz dönüştürücülerde geleneksel yükseltici GFD konvertörlerde bulunan köprü doğrultucu ortadan kaldırılmıştır. Önerilen algoritmada iç akım kontrol döngüsü ile aktif ve reaktif güç kontrol edilmiştir. İç kontrol döngüsünde yenilikçi filtreleme ve sinyal işleme yöntemleri kullanılarak referans akım hesaplanmıştır. İç akım döngüsü PI kontrolör kullanarak PWM anahtarlama sinyallerini üretmektedir. Önerilen kontrol tekniğinin analitik analizi detaylı olarak sunulmuştur. Önerilen kontrolörün performansı PSIM devre simülasyonları kullanılarak 300W dönüştürücü için doğrulanmıştır.

Anahtar Kelimeler: Köprüsüz boost doğrultucu, Güç faktörü düzeltici PFC, Güç kalitesi, Toplam harmonik bozulma, PQ teori

1. Introduction

From the perspective of environmental protection and restricted reserves of conventional fuels, renewable energy (RE) systems, such as photo voltaics (PV), wind, and micro turbines are expected to rise (Marei et al. 2002). The increasing presence of nonlinear loads, such as variable speed controllers, light emitting diode (LED), uncontrolled rectifier loads, and other switching equipment will further reduce Distributed Generation DG system power quality (Bojoi et al. 2011, He et al. 2014). These loads produce harmonics and reactive power in the DG systems. The existence of harmonics in the DG systems ends up with some impacts, including increased heat losses in transformers, electrical motors, and power lines; low power factor; insufficient usage of distribution cable and plant. Conventional passive filters PF have been used in order to meet the standards such as IEEE-519 and IEC-555, to compensate DG systems harmonics, and to develop power quality, but are often not ideal due to increased cost, fixed compensation, large size, and resonance problems (Akagi et al. 2007).

Recently, power factor correction (PFC) rectifiers are included as aninherent part of the AC-DC transformation systems. PFC rectifierseliminate harmonics at the input

*Corresponding author: yasemin.onal@bilecik.edu.tr

Yasemin Önal orcid.org/0000-0003-0173-0948

current, improve output of the rectifier, and obtain higher efficiency with a reduced size. Different PFC techniques are used to obviate power quality problems. Among these, the boost rectifier topology has been comprehensively used in different AC-DC for PFC rectifiers. Bridgeless boost PFC (BBPFC) rectifier has been improved to minimize the rectifier bridge conduction loss. The BBPFC rectifier does not utilize bridge diodes, consequently decrease switch in circuit current way in contrast to the conventional boost PFC rectifier. This is especially advantageous when the rectifier activates with nominal voltage line entries. Transmission losses by the switches can be further reduced through holding the non- controlled switch on (Huber et al. 2008, Gopinanth et al. 2011).

In the literature, the output voltage and input current can be controlled in PFC rectifiers by using some different control algorithms for improved THD and corrected PF in PFC rectifiers. These control algorithms are average current control, predictive current control, and other complicated controllers. In the average current control strategy, the reference of the inner current loop is obtained by multiplying the output of the outer loop by the sensed input voltage (Leon-Masich et al. 2014, Ji et al. 2015, Marcos-Pastor et al. 2016). This is the strategy used in studies that improved a hysteretic current controller as the inner control loop because of its stability and dynamic response. The predictive current control algorithm predicts the current of the next-state based on the current of the current state due to the optimal duty cycle obtained by minimizing the error between the reference current and the estimated current. (Monteiro et al. 2016, Park et al. 2016, Yang et al. 2016).

Running BBPFC rectifiers is expected to reduce the total harmonic distortion (THD) in order to meet the standards. It is difficult to meet the THD necessities with the existing control techniques. Active and reactive (*pq*) control theory was originally improved for active power filtering of the multi phase systems, which is the proper methodology of producing signals (Akagi et al. 1984). Khadkikar et al. (2009) have ably expanded the term of active and reactive power dispersion in a □b coordinates for a single-phase system. Having successful THD reduction for active power filtering practices motivated us to use the *pq* theory in controlling the bridgeless PFC controllers.

This study presents a new controller for BBPFC rectifiers, which reduces the THD and improves the PF of the operation. The input rectifier bridge in conventional boost PFC (CBPFC) rectifiers are discarded in bridgeless rectifiers to reduce complexity and increase the overall efficiency. The success of the improved controller is confirmed for 300W rectifier using PSIM circuit simulations. Section 2 presents the available bridgeless boost PFC circuit topology. The derivation of the *pq* control method for bridgeless PFC rectifier is presented in Section 3. The simulation results of the conventional and *pq* control are presented in Section 4. Conclusion is provided in Section 5.

2. Material and Methods

Figure 1 shows the block diagram for the generation of the reference current, based on the *pq* controller. The instantaneous reactive power method or *pq* method is one of the most proper methodologies to obtain instantaneous reference signals for the bridgeless PFC rectifier.

This method was originally developed for 3-phase systems. The *pq* method cannot be applied directly to single phase systems and some transformation needs to be done before application to single phase systems. Lately, the 3-phase *pq* method was expanded for single phase systems such that the benefits of the 3-phase *pq* method can be used in single phase systems as well. Moreover, the fact that the single phase *pq* method can be well applied to 3-phase systems gains advantage over the 3-phase method under the influence of unbalanced conditions, and further, it generates a sinusoidal source current under unbalanced source voltages and load conditions (Haque 2002). The single phase *pq* method is based on an instantaneous $\pi/2$ lag or $\pi/2$ lead of current and voltage to define the original system as a 2-phase system. Thus, the overall system can be easily represented in α and β coordinates. The original source voltage and load current are considered as quantities on the a-axis, whereas b-axis quantities are obtained by a $\pi/2$ lag or $\pi/2$ lead of the source voltage and load current (Zeng et al. 2014, Song et al. 2014).

$$\begin{aligned} v_\alpha &= v = V_m \sin(\ t\ ) \\ v_\beta &= v(t+(\pi/2)) = V_m \cos(\ t\ ) \end{aligned} \tag{1}$$

Similarly, the source current description in α and β coordinates with a $\pi/2$ lead imaginary part of $i(t)$, respectively.

$$\begin{aligned} i_\alpha &= i(t+\varphi_s) \\ i_\beta &= i(t+\varphi_s+(\pi/2)) \end{aligned} \tag{2}$$

The single phase p and q power, as described in the main 3-phase *pq* control method, can be described in (3)

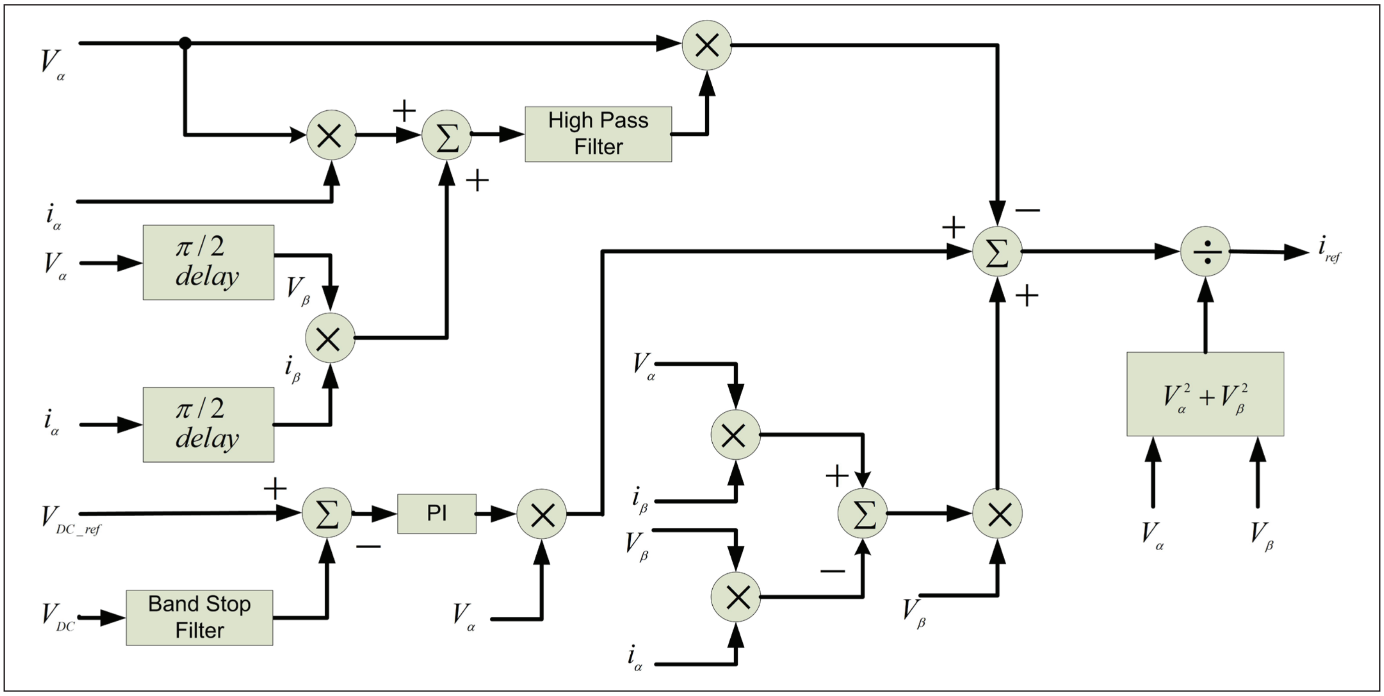

Figure 1. Improved controller schema for bridgeless PFC rectifier.

$$\begin{aligned} p &= v_\alpha \times i_\alpha + v_\beta \times i_\beta \\ q &= -v_\beta \times i_\alpha + v_\alpha \times i_\beta \end{aligned} \tag{3}$$

The p and q can be represented in (4)

$$\begin{aligned} p &= \bar{p} + \tilde{\tilde{p}} \\ q &= \bar{q} + \tilde{\tilde{q}} \end{aligned} \tag{4}$$

where $\bar{p}$ and $\bar{q}$ describe the direct current constituents accountable to base p and q power, while $\tilde{\tilde{p}}$ and $\tilde{\tilde{q}}$ describe the alternative current constituents accountable for the reactive power. (4) can be rewritten as shown in (5).

$$\begin{aligned} p &= v_\alpha \times i_\alpha + v_\beta \times i_\beta = \bar{p} + \tilde{\tilde{p}} \\ q &= -v_\beta \times i_\alpha + v_\alpha \times i_\beta = \bar{q} + \tilde{\tilde{q}} \end{aligned} \tag{5}$$

PFC rectifier should produce a current to eliminate the harmonics produced by a single phase DC, and besides, should equalize harmonic power needed for the load. Control current should be the total of the reactive current and harmonic current.

The high frequency switching of the rectifier generates switching ripples on the DC load. The switching ripples can introduce an error in reference signal estimation. Therefore, the sensed DC output voltage is processed by using a band stop filter BSF before comparison with the reference value and $\bar{p}_{dc}$ loss power is obtained.

The notation $\tilde{\tilde{p}}$ can be obtained easily from p by using a high pass filter HPF. The reference current should be predicated on $\tilde{\tilde{p}}, q$ and $\bar{p}_{dc}$. The reference current can be described by (6)

$$\begin{aligned} i_{ref} &= (1/v_\alpha^2 + v_\beta^2) \times v_\alpha \times (-\tilde{\tilde{p}}) + v_\alpha \times \overline{p}_{dc} + v_\beta \times q) \\ &= (1/A) \times v_\alpha \times (-\tilde{\tilde{p}}) + v_\alpha \times \overline{p}_{dc} + v_\beta \times q) \end{aligned} \tag{6}$$

The obtained reference current signal is compared to the sensed source current in the current control loop and PWM switching signals are generated.

3. Bridgeless Boost PFC Rectifier

A bridgeless PFC rectifier is advanced by a small development in the Conventional Bridgeless PFC rectifier. The bridgeless PFC rectifier attracts more attention for its ability to decrease transmission losses.

3.1. Circuit topology

Figure 2 shows the schema of a BBPFC rectifier circuit (Su et al. 2011, Muhammad and Lu 2012, Santos and Barrero 2013, Lu et al. 2015, Musavi et al. 2011, Cho 2014). As exhibited in Figure 3, there is one active switch at each half cycle. Each operating cell consists of an active and a passive switch. Q_1 active switch and D_1 passive switch operate in switching cycle to the half line cycle, when link L line is high and Q_2's body diode is conducted as current back path. The negative cycle, Q_2 active switch, and D_2 passive switch operate as switching cycle, when the link N line is high, and the Q_1's passive switch is conducted as current back path.

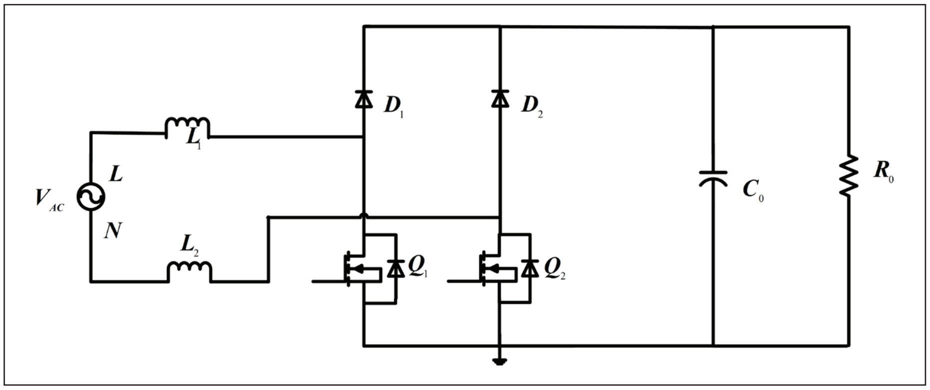

Figure 2. Bridgeless boost PFC rectifier circuit.

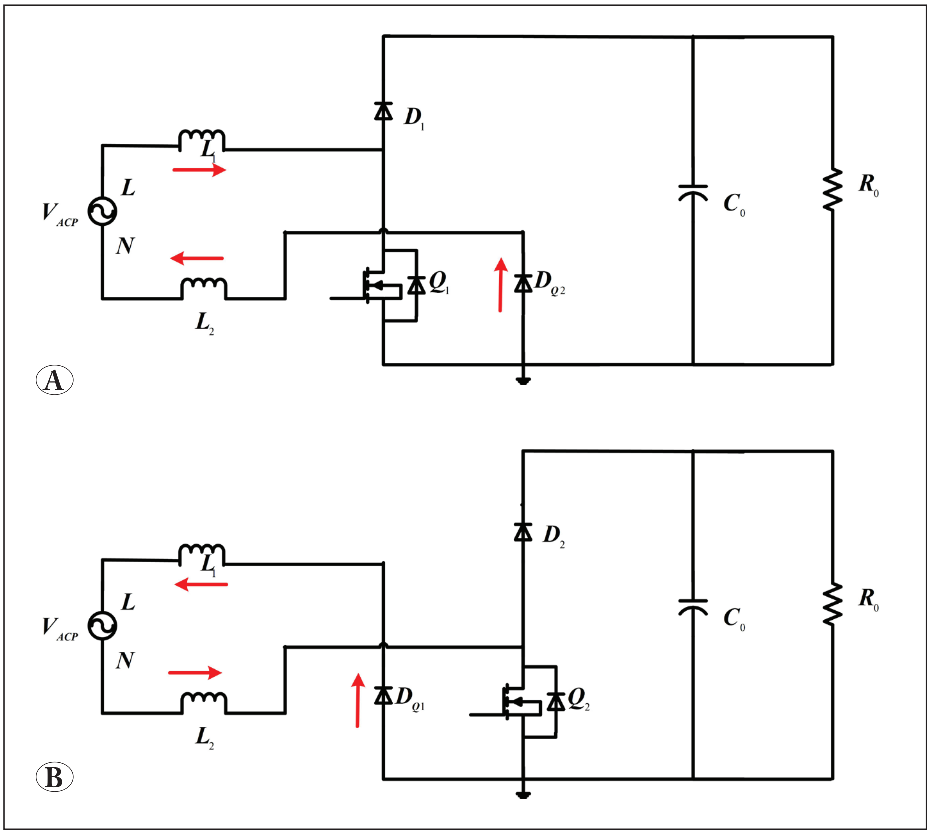

Figure 3. Bridgeless boost BPFC rectifier operation mode with **(A)** positive and **(B)** negative line cycle.

The losses due to bridge rectifier are eliminated in contrast to a CBPFC rectifier circuit. There is only one passive switch transmission loss for a BPFC rectifier opposite to the transmission loss out of two passive switches in a CBPFC rectifier. It can enhance productivity by removing the voltage decline of one passive switch in the current route (Xue and ZhiHao 2009) (Xue and ZhiHao 2009).

3.2. Circuit parameters

Followings are the standard equations to create the main components of the AC-DC BBPFC rectifier. The design is explicated in (Ekemezie 2007, Todd 1999). There are many other factors contained in the create process of 300W BBPFC rectifier. Source voltage effective is in the range of 85V-265V AC, DC voltage is 400V DC, source frequency is 60Hz and the operation frequency is 75kHz. Target efficiency is 0.95. To element choose on the BBPFC rectifier, supposing the maximum source current is adjust to %20 of the peak source current, the next computations are utilized to choose the proper L_1 and L_2. inductance value. Where, variance D_{PLL} is the rectifier's duty cycle at the peak of negative line process. Δ_{IL} is the boost inductor oscillation current at the peak of negative line attributed on the rectifiers source oscillate current necessities. D_{PLL} is computed from (7) for $P_{OUT} = 300W$

$$D_{PLL} = \left(V_{OUT} - V_{IN\_\min}\sqrt{2}\right)/V_{OUT} = \left(400 - 85\sqrt{2}\right)/400 \approx 0.7 \tag{7}$$

Inductor ripple current is calculated from (8)

$$\begin{aligned}
\Delta I_{IL} &= \frac{P_{OUT}\times\sqrt{2}\times 0.2}{V_{IN_\min}\times\eta} = \frac{300W\times\sqrt{2}\times 0.2}{85V\times 0.95} = 1.05A \\
I_{IN_peak} &= \frac{P_{OUT}\times\sqrt{2}}{V_{IN_\min}\times\eta} = \frac{300W\times\sqrt{2}}{85V\times 0.95} = 5.24A \\
\Delta I_{L_peak} &= \frac{P_{OUT}\times\sqrt{2}}{V_{IN_\min}\times\eta} + \frac{\Delta I_L}{2} = \frac{300W\times\sqrt{2}}{85V\times 0.95} + \frac{1.05}{2} = 5.764A
\end{aligned} \tag{8}$$

The minimum inductor at negative line can be computed as shown in (9).

$$\begin{aligned}
L1_{\min} = L2_{\min} &= \frac{V_{IN_\min}\times\sqrt{2}\times D_{PLL}}{\Delta I_L \times f_s} = \frac{85\times\sqrt{2}\times 0.7}{1.05\times 75kHz} \\
&= 1.07mH
\end{aligned} \tag{9}$$

The out capacitance C_0 chosen is attributed to hold up requirements as demonstrated in (10).

$$\begin{aligned}
C_0 &\geq \frac{P_{OUT}}{2\times\pi\times f_{line}\times V_{OUT}^2\times\Delta V_{0_ripple}} \\
&= \frac{300}{2\times\pi\times 60\times 400^2\times 0.03} = 165.87\mu F
\end{aligned} \tag{10}$$

where ΔV_{0_ripple} is the desired peak to peak DC voltage oscillate and is regarded as %30 in this design. The out C_0 by %20 allowance so as to guarantee least capacitance necessities are contented in (11).

$$C_0 \geq \frac{C_{0\_\min}}{1-0.2} = \frac{165.87\mu F}{0.8} \geq 207.33\mu F \tag{11}$$

4. Conclusions

The parameters of the power circuits for bridgeless boost PFC rectifier are described in Table 1. The improved *pq* controller is simulated to verify the productivity of a single-phase BBPFC rectifier. The PSIM simulation software has been used for this purpose. The simulation results are exhibited in Figure 4-9.

Table 1. The Simulation Parameters

Input inductances L_1,L_2(mH)	1.1
Output capacitance Co(µF)	250
Source voltage V_{rms}(V)	120
Rated output power P_o (W)	300
Output voltage V_{dc} (V)	400
Operating frequency f_{line}(Hz)	60
Switching frequency f_s(kHz)	75

4.1. PSIM simulation of bridgeless boost PFC with the avarage current control strategy

The bridgeless boost PFC is simulated by using the parameters exhibited in Table 1. Figure 4 shows the PSIM simulation circuits with average current control.

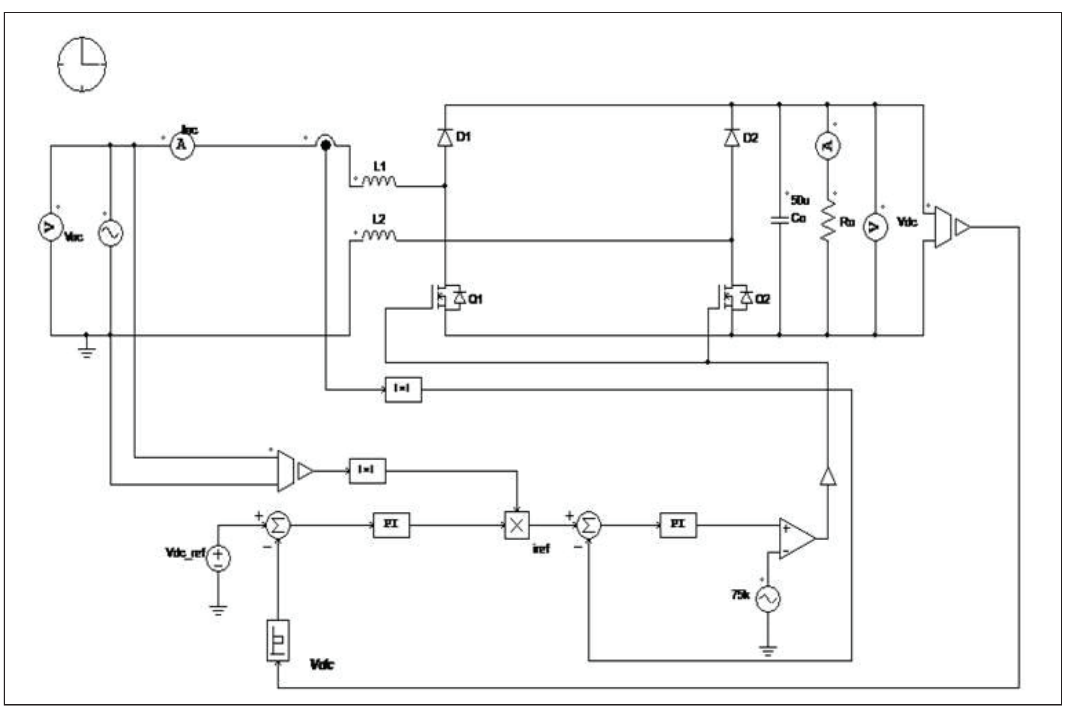

Figure 4. PSIM simulation circuit for 300W BBPFC rectifier with average current control.

It comprises of a current loop and a voltage loop. The sensed input voltage is multiplied by the compensated output voltage. It, next, produces a control signal contrasting with the switching signal to produce the gating signals for Mosfet. The average current control strategy is used for the bridgeless boost PFC converter, as outer voltage controller generates the reference current to regulate the DC voltage and as the inner PI controller generates the gating signals. The high frequency switching of the converter produces switching ripples on the DC voltage. Thus, the measured DC voltage is processed through a band stop filter to eliminate the noise on the measurements.

Figure 5 shows the transient input voltage, input current, output voltage, output current, and output power for 300W BBPFC rectifier with average current control.

Figure 6 demonstrates the input voltage and input current, output voltage waveforms for 300W BBPFC rectifier with average current control. It can be seen from Figure 6 that the input current is in phase with input voltage and is sinusoidal with THD %5.51 and PF 0.9894 values. Output voltage is obtained at about 400V with a 120Hz frequency ripple.

4.2. PSIM simulation of bridgeless boost PFC rectifier with the improved control algorithm

Table 1 shows the parameters that are used to simulate

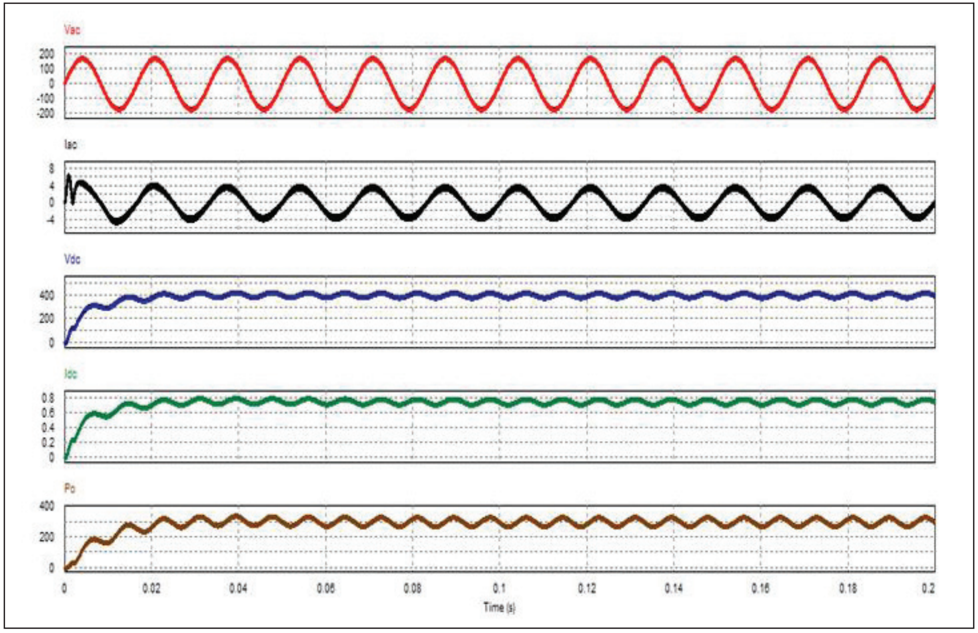

Figure 5. The transient input voltage, input current, output voltage, output current and output power for 300W BBPFC rectifier with average current control.

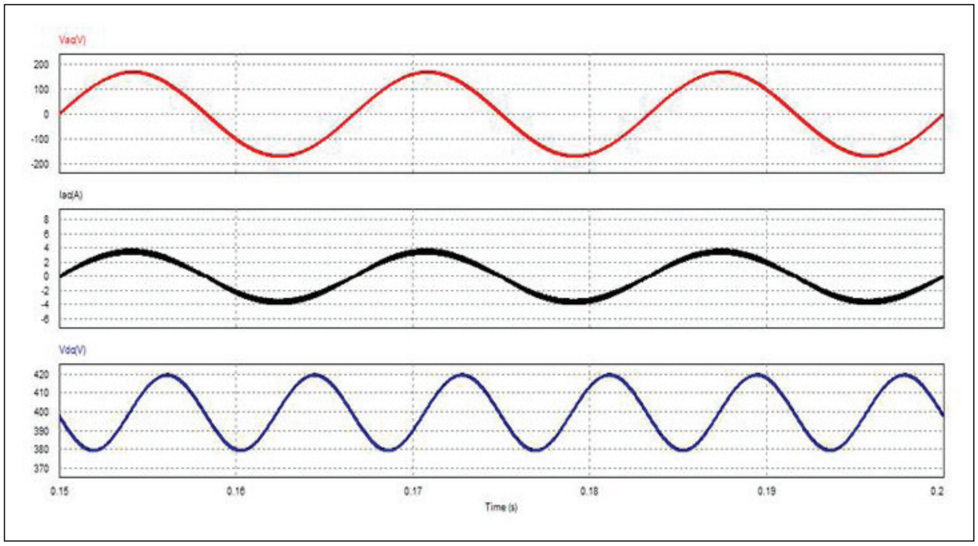

Figure 6. The input voltage and current, output voltage waveforms for 300W BBPFC rectifier with average current control (PF 0.9894, THD %5.51).

the BBPFC rectifier. The PSIM simulation through *pq* algorithm is exhibited in Figure 7.

The i_{ref} should be calculated by $q, \bar{p}_{dc}$ and $\tilde{\tilde{p}}$. The notation $\tilde{\tilde{p}}$ can be easily obtained from p by use of a high-pass filter. The high f_s operation of the rectifier reasons pulsing fluctuations on the out voltage signal. These switching oscillations can produce a mistake. So, the perceived DC link voltage is processed by use of a band stop filter before contrasting with the reference value. Figure 8 presents the transient input voltage, input current, output voltage, output current, and output power for the 300W BBPFC rectifier with improved *pq* controller.

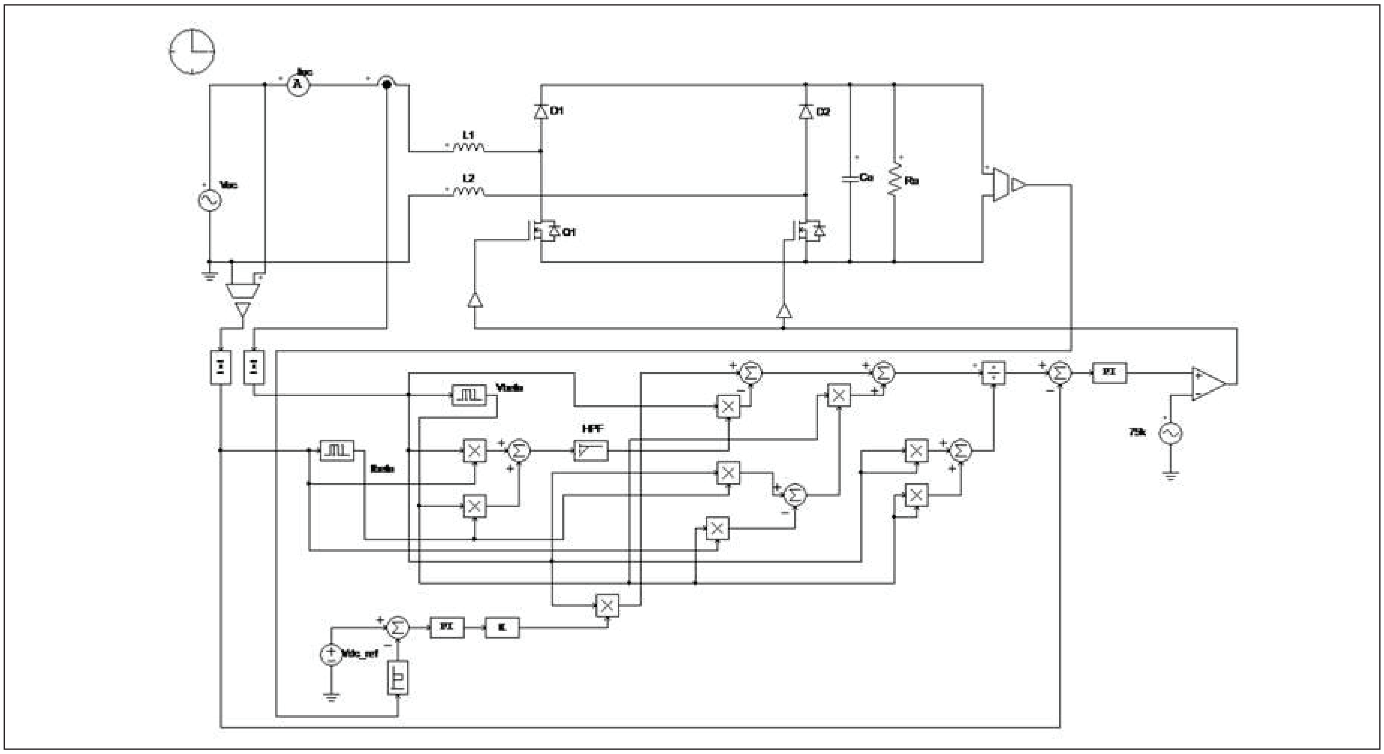

Figure 7. PSIM simulation circuit for 300W BBPFC rectifier with *pq* controller.

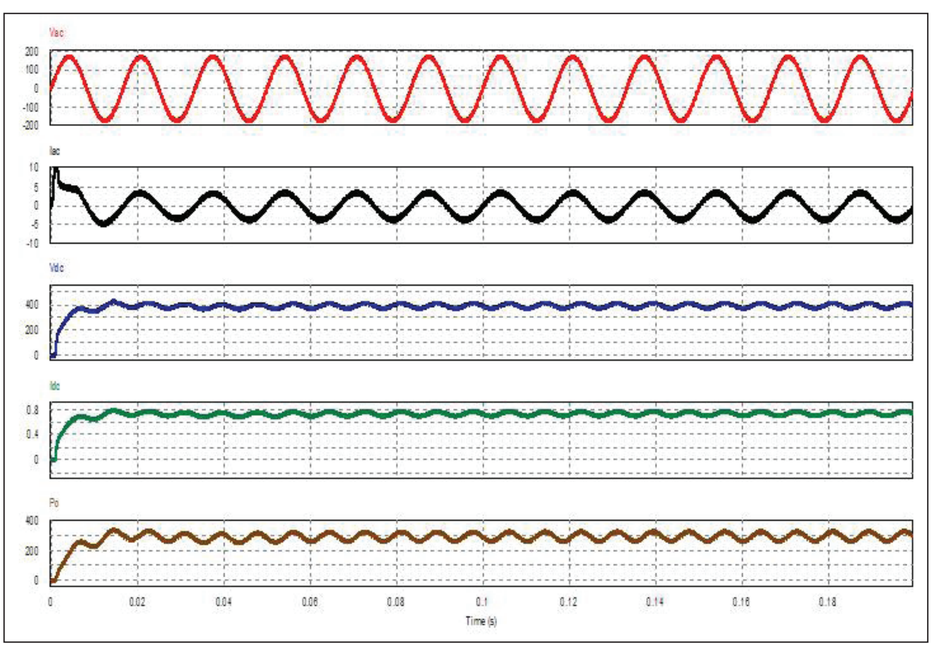

Figure 8. The transient signals for 300W BBPFC rectifier with improved *pq* controller.

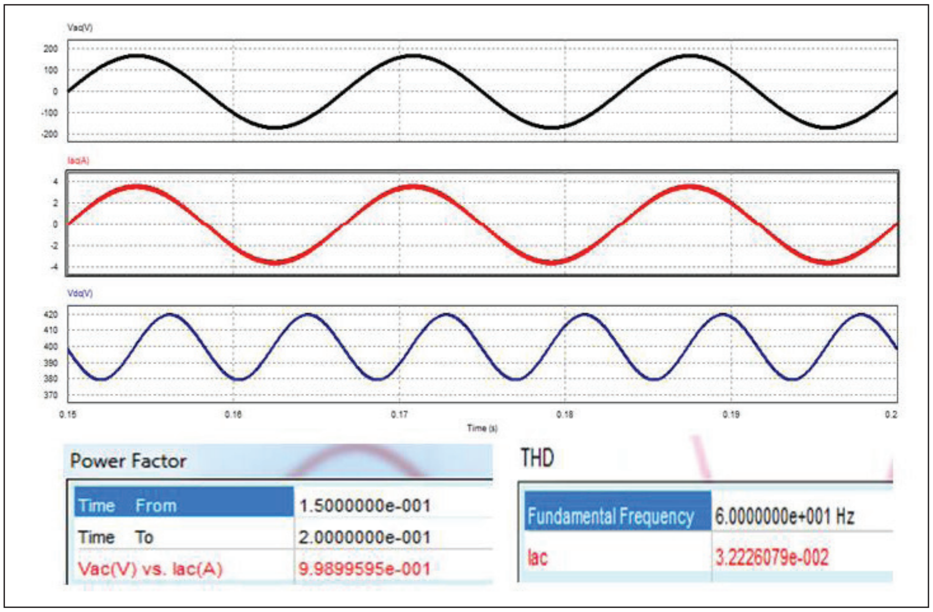

Figure 9. The input voltage and current, output voltage waveforms for 300W BBPFC rectifier with improved *pq* controller (PF 0.9989, THD %3.22).

Figure 9 presents the input voltage and input current for the improved *pq* controller. It can be seen from Figure 9 that input current is in phase with input voltage and is sinusoidal with low THD (%3.22) and high PF (0.9989) values. Output voltage is obtained at about 400V, with a 120Hz low frequency ripple.

4. Discussion

In this paper, a new controller is developed for a single phase bridgeless BPFC rectifier, using *pq* power control. The improved controller calculates the active and reactive powers and generates reference current signals through filtering and signal processing techniques. Through simulation, the performance of the improved control method is compared with that of the average current control method. The improved *pq* controller is implemented on a 300 W rectifier operating from 120V AC source to generate 400V DC output.

The improved controller is able to reduce the THD to %3.22 from %5.51, and improve the power factor to 0.9989. When some of BPFC control methods are compared in Table 2, the simulations show that it is a perfect choice to improve *pq* controller for single phase BBPFC rectifier algorithm solution for lower power applications especially for those which require high quality input power.

Table 2. The comparison of control methods in terms of THD and PF.

	THD (%)	PF
Average current controller	5.51	0.9894
Improved *pq* controller	3.22	0.9989

5. References

Akagi, H., Kanazawa, Y., Nabae, A. 1984. Instantaneous reactive power compensators comprising switching devices without energy storage components. *IEEE Trans. Ind. Applicat.*, 20(3): 625-630.

Akagi, H., Watanabe, E.H, Aredes, M. 2007. Instantaneous Power Theory and Applications to Power Conditioning. 2nd ed, Wiley, New Jersey, USA. 379 pp.

Bojoi, R.I, Limongi, L.R, Roiu, D. 2011. Enhanced power quality control strategy for single-phase inverters in distributed generation systems. *IEEE Trans. Power Electron.*, 26: 789-806.

Cho, Y. 2014. A Low Cost Single-Switch Bridgeless Boost PFC Converter. *International Journal of Power Electronics and Drive Systems,* 4(2):256-264.

Ekemezie, PN. 2007. Design of a power factor correction ac-dc converter. IEEE, pp.1-8, *AFRICON.*

Gopinanth, M., Prabakaran R., S. 2011. A brief analysis on bridgeless boost PFC converter. *IET 2011 Sustainable Energy and Intelligent Systems Conference,* pp.242-246, Chennai.

Haque, MT. 2002. Single-phase PQ theory for active filters. *IEEE 2002 Power Electronics Specialists Conference,* pp. 1941-1944, Caims, Qld.

He, J., Li, YW., Blaabjerg, F. 2014. Active harmonic filtering using current-controlled, grid-connected DG units with closed-loop power control. *IEEE Trans. Power Electron.,* 29: 642-653.

Huber, L., Jang, Y., Jovanovic, MM. 2008. Performance evaluation of bridgeless PFC boost rectifiers. *IEEE Trans. Power Electron.,* 23(3): 1381-1390.

Ji, Q., Ruan X, Xie, L., Ye, Z. 2015. Conducted EMI spectra of average current controlled boost PFC converters operating in both CCM and DCM. *IEEE Trans. Ind. Electron.,* 62: 2184–2194.

Khadkikar, V., Chandra, A., Singh, BN. 2009. Generalised single-phase p-q theory for active power filtering: Simulation and DSP-based experimental investigation. *IET Power Electron,* 2: 67-78.

Leon-Masich, A., Valderrama-Blavi, H., Bosque-Moncusi, JM., Martinez-Salamero, L. 2014. A high voltage SiC-based boost PFC for LED applications. *Proc. 9th Int. Conf. Ecological Vehicles Renew. Energies (EVER),* pp.1-5, Monte-Carlo, Monaco.

Lu, B., Brown, R., Soldano, M. 2005. Bridgeless PFC implementation using one cycle control technique. *IEEE 2005 Appl. Power Electron. Conference and Exposition,* pp. 812-817, Austin TX.

Marcos-Pastor, A., Vidal-Idiarte, E., Cid-pastor, A., MartinezSalamero, L. 2016. Interleaved digital power factor correction based on the sliding-mode approach. *IEEE Trans. Power Electron.*, 31: 4641–4653.

Marei, MI., El-Saadany, EF., Salama, MMA. 2002. Flexible distributed generation:(FDG). *IEEE Power Engineering Society Summer Meeting Conference,*pp. 25-26, Chicago, USA.

Marques, GD., 2000. An instantaneous active and reactive current component method for active filters. *IEEE Trans. Power Electron.,* 15(4): 660-669.

Monteiro, V., Nogueiras Meléndez, AA., Couto, C., Afonso, JL., 2016. Model predictive current control of a proposed single-switch three-level active rectifier applied to EV battery chargers. *Industrial Electronics Society IECON 2016–42nd Annual Conference of the IEEE*, pp.1365-1370, Florence, Italy.

Muhammad, KS., Lu, DDC. 2012. Two-switch ZCS totem-pole bridgeless PFC boost rectifier. *IEEE 2012 Power and Energy International Conference*, pp. 1-6, Kota, Kinabalu.

Musavi, F., Eberle, W., Dunford, WG. 2011. A phase shifted semi-bridgeless boost power factor corrected converter for plug-in hybrid electric vehicle battery chargers. *IEEE 2011 Appl. Power Electron. Conf. and Expo,* pp. 821-828, Fort Worth.

Park, JH., Kim, DJ., Lee, KB. 2016. Predictive control algorithm including conduction-mode detection for PFC converter. *IEEE Trans. Ind. Electron.,* 63: 5900–5911.

Santos, OL., Barrero, JM. 2013. Digitally implemented sliding-mode control of a single-phase dual-boost PFC rectifier. *IEEE 2013 Power Electronics and Power Quality Applications Conference,* pp. 1-5, Bogota.

Song, X., Xijun, N., Huang, AQ. 2014. Selected harmonic resistance control based series active power filter. *IEEE 2014 Energy Conversion Congress and Exposition,* pp. 3449-3455, Pittsburgh, PA.

Su, B., Zhang, JM., ZY, Lu., 2011. Totem-Pole Boost Bridgeless PFC Rectifier With Simple Zero-Current Detection and Full Range ZVS Operating at the Boundary of DCM/CCM. *IEEE Trans. on Power Electron.,* 26: 427-435.

Todd, PC.1999. Boost power factor correction design with the UC3853. Unitrode Corporation Application note, Marrimach, NH, 22.

Yang, SH., Meng, CH., Chiu, CC., Chang, CW., Chen, KH., Lin, YH., Lin, SR., Tsai, TY. 2016. A buck power factor correction converter with predictive quadratic sinusoidal current modulation and line voltage reconstruction. *IEEE Trans. Ind. Electron.*, 63: 5912–5920.

Xue, CL., Soares, V., Verdelho, P., ZhiHao, W. 2009. UCC28070 Implement Bridgeless Power Factor Correction (PFC) Pre-Regulator Design. Application Report of Texas Instruments, SLUA517, Dallas, Texas, USA.

Zeng, Z., Yang, J., Chen, S. 2014. Reduced order generalized integrators based selective harmonic compensation current controller for shunt active power filters. *IEEE 2014 Energy Conversion Congress and Exposition.* pp. 1650-1655, Pittsburgh, PA.